Investigating the downstream sediment load change by an index coupling effective rainfall information with reservoir sediment trapping capacity

Rongrong Li[a], *Lihua Xiong*[a,*], *Bin Xiong*[a], *Yu Li*[b], *Quanxi Xu*[b], *Lei Cheng*[a], *Chong-Yu Xu*[c]

[a]*State Key Laboratory of Water Resources and Hydropower Engineering Science, Wuhan University, Wuhan 430072, China*

[b]*Bureau of Hydrology, Changjiang Water Resources Commission, Wuhan 430010, China*

[c]*Department of Geosciences, University of Oslo, P.O. Box 1022 Blindern, 0315 Oslo, Norway*

E-mail addresses:

R. Li (*lirongrong@whu.edu.cn*)

L. Xiong (*xionglh@whu.edu.cn*)

B. Xiong (*xiongbin@whu.edu.cn*)

Y. Li (*liyuwhu@163.com*)

Q. Xu (*xuqx@cjh.com.cn*)

L. Cheng (*lei.cheng@whu.edu.cn*)

C-Y. Xu (*c.y.xu@geo.uio.no*)

**Corresponding author*:

Lihua Xiong, PhD, Professor

State Key Laboratory of Water Resources and Hydropower Engineering Science

Wuhan University, Wuhan 430072, P.R. China

E-mail: *xionglh@whu.edu.cn*

Telephone: *+86-13871078660*

Fax: *+86-27-68773568*

Abstract

Sediment load is a critical issue in hydrologic process analysis and river basin management. Many studies have analyzed the impacts of rainfall or reservoir separately on the downstream sediment load; however, few researches investigated the coupled effect of rainfall and reservoir on sediment load change. In this study, a rainfall-augmented sediment trapping index (RSTI) that combines the impacts of effective rainfall and reservoir sediment trapping capacity was developed to attribute the sediment load change in the Wujiang River Basin (WRB) during the period of 1952-2017. Eight linear or nonlinear regression models were set up to investigate how to best utilize the proposed RSTI to reveal the coupled effect of rainfall and reservoir on the downstream sediment load of WRB. It is found that observed sediment load has a large decrease after 1984 when the Wujiangdu Reservoir was put into full operation while rainfall had only a slight change in the same period. The nonlinear regression model with RSTI as an explanatory variable (NSE = 0.837) has the best performance in simulating the observed sediment load series. These results might be helpful for the downstream sediment management under a changing environment.

Keywords: sediment load; rainfall and reservoir; RSTI; eight linear or nonlinear regression models; Wujiang River

1 Introduction

Sediment transport and deposition play a dominant role in the formation of geomorphology and the evolution of the earth ecology. Sediment is defined as solid particles in natural water body, which mainly comes from the erosion of water flow to the surface in the basin (Huang *et al*., 2017; Pelletier, 2012). As a crucial factor of river evolution, excessive sediment concentration may lead to problems such as the water quality deterioration of rivers, channel filling and reservoir deposition, while deficient sediment concentration causes erosion and retreat in the lower estuary delta (Singh, 1995; Syvitski and Milliman, 2007). In addition, sediment plays a very important role in water and sediment resource management, water conservancy project construction, ecological environment improvement, and national economic development (Miao *et al*., 2011; Peng *et al*., 2010).

Identifying the driving force leading to the change of sediment load has received more and more attention from researchers around the world in recent years. The climate dominates the process of sediment yield (e.g. sediment yield due to rainfall erosion and wind erosion) (Lal, 1994; Wu *et al*., 2018a; Xu, 2003; Zhu *et al*., 2008), human activities (e.g. the reservoirs can intercept sediment; the effect of vegetation on sediment is wind proofing and sand fixing) (Wu *et al*., 2018b; Xu, 2007; Xu *et al*., 2018; Yang *et al*., 2002; Zhang *et al*., 2018) directly influence the process of sediment transport. Among the various driving factors for the production and transport of sediment, rainfall erosion and reservoir interception are the most significant ones, which have been widely concerned by scholars (Rossi *et al*., 2009; Walling, 2006; Yang *et al*., 2006). Sediment formation comes directly from soil erosion, which generally goes through the following processes: raindrop splash, separation of soil particles, runoff erosion and transportation, and soil loss. The changes of rainfall may have extensive effects on sediment generation and transportation (Zhu *et al*., 2008). Xu (2003) found that the dramatic reduction in sediment flux from the Yellow River to the sea could be attributed to the change in rainfall. Lu *et al*. (2013) indicated that every 1% change in rainfall could result in 2% change in sediment load. After the construction of many large reservoirs, the Nile (Wiegel, 1996) and the Colorado (Carriquiry and Sanchez, 1999) rivers have lost almost 100% of their sediment flux. Yang *et al*. (2002) illustrated that sediment discharge of the Yangtze River reduced by 34% as a result of human activities, especially reservoir construction. And the sediment discharge decreased significantly due to the construction of cascade reservoirs (Wu *et al*., 2018b). In addition, rainfall directly affects the regulation and storage management of reservoirs. Therefore, quantitative identification of the impacts of rainfall and reservoir on the non-stationarity of the sediment load series is helpful to understand the dynamic process of sediment production and transport in the basin under a changing environment (Lu *et al*., 2013; Wen *et al*., 2019).

In studying the relationship between a hydrological dependent variable such as sediment load and its explanatory variables or influencing factors, the regression method gets a widespread use for its simplicity and applicability. Bezak *et al*. (2017) used the precipitation sum and the peak discharge as covariates to estimate the suspended sediment load with regression models. Wen *et al*. (2019) established the multiple linear regression equation of areal rainfall amount and annual sediment load to illustrate the effect of climate variability on sediment load change. Uca *et al*. (2018) carried out the multiple linear regression analysis to correlate the measured suspended sediment to the independent variables, namely discharge, rainfall, and water depth.

However, there are two concerns with the utilization of regression methods in studying sediment load. The first concern is that they have focused more on establishing the linear relationship between the hydrological dependent variables and the selected explanatory variables. It is obvious that the nonlinear model is more suitable to describe the relationship between hydrological variable and its influencing factors due to the nonlinear characteristics of hydrological system. The second concern is that the interaction between different factors in controlling the sediment load was ignored. Hydrological processes are complex and dynamic processes influenced by many factors simultaneously. So, it is especially necessary to consider the coupling effects between different influencing factors such as rainfall and reservoirs. For example, Xiong *et al*. (2019) defined the rainfall-reservoir composite index (RRCI) to carry out the non-stationarity frequency analysis of downstream flood, their results indicate that the impact of reservoir on flood is related not only to static reservoir storage capacity but also to dynamic reservoir operation influenced by multiday antecedent rainfall input. Similarly, the downstream sediment load of dams is a coupled outcome of the antecedent rainfall and reservoir size. How to construct a composite index to explain the coupled impact of rainfall and reservoir on the sediment load process is to be explored.

As the largest tributary of the upper reaches of the Yangtze River, the Wujiang River Basin (WRB) is one of the main sediment sources of the Yangtze River (Xu, 2009), there are 22.5 million tons of sediment inflow to the basin mouth every year. Xu (2007) studied the decreasing trend in grain size of suspended sediment load at Wulong station of the Wujiang River. Then, Xu (2009) analyzed the impact of human activities including reservoir construction on the variation of suspended sediment concentration qualitatively. Wu *et al*. (2018b) demonstrated the cascade dam effects on sediment by observing the process of annual sediment discharge before and after the reservoir construction. These studies emphasized the inter-annual variation of sediment in the Wujiang River before and after the construction of large reservoirs, but didn't carry out quantitative identification of physical causes for the variation of sediment in the WRB.

The major objectives of this paper are as follows: (1) analyze the variation of long-term historical records of sediment load in the WRB; (2) develop the rainfall-augmented sediment trapping index (RSTI) that couples the impacts of both effective rainfall and sediment trapping capacity of reservoirs; and (3) compare the simulated sediment load of eight linear or nonlinear regression models to reveal the coupled effect of rainfall and reservoir on sediment load, so as to obtain the optimal quantitative relationship between rainfall, reservoir and sediment load.

The rest of this paper is organized as follows: the study area and data used in this study are introduced in the next section; Section 3 describes the methodology used in this study; the results of this study are presented in Section 4; in Section 5 some discussions are described, and the main conclusions are summarized in Section 6.

2 Study area and data

2.1 Study area

The Wujiang River Basin (WRB) is situated between 104°18′E-109°22′E and 26°07′N-30°22′N, covering a total area of 87920 km^2 (**Figure 1**). It is the largest tributary in the upper reaches of the Yangtze River in China measuring approximately 1050 km in length, so it has a great contribution to the water and sediment of the Yangtze River. The Sancha River in the south source and the Liuchong River in the north source are considered as main soil erosion areas in the WRB. The basin belongs to subtropical monsoon climate with the flood season from May-October and non-flood season from November-April. The mean annual rainfall varies between 800-1700 mm during the period of 1952-2017. The river has a mean annual runoff of 487×10^8 m^3 and a mean annual sediment load of 2252×10^4 t for the period of 1952-2017 at the Wulong hydrological station (with a drainage area of 83035 km^2). Many reservoirs have been built in the basin, and the information of all 11 reservoirs on the main stream of the WRB (Wu *et al.*, 2018b) has been listed in **Table 1**. Annual sediment trapping of reservoirs is obtained by statistics of measured data (Chen *et al.*, 2008), among them, sediment trapping of Suofengying, Yinzidu and Puding reservoirs is estimated based on the Brune method (Brune, 1953).

< Figure 1>

< Table 1>

2.2 Data

In this study, daily runoff and sediment load records (1952-2017) from the Wulong station and reservoir data in the WRB are provided by the Hydrology Bureau of the Changjiang Water Resources Commission, China (http://www.cjh.com.cn/en/). The rainfall data based on the records of 15 meteorological sites (shown in **Figure 1**) are obtained from the National Climate Center of the China Meteorological Administration (http://data.cma.cn/site/index.html), mean rainfall data of 15 stations are presented in **Table 2**. Annual normalized difference vegetation index (NDVI) (1982-2015) is downloaded from Landsat NDVI (https://ecocast.arc.nasa.gov/data/pub/gimms/). Land-use and land-cover change (LUCC) for 1980 and 1990 are obtained from Resource and Environment Data Cloud Platform, China (http://www.resdc.cn/Default.aspx).

< Table 2>

3 Methodology

In this section, first, the Mann-Kendall test and Pettitt test are used to detect the trend and change-point of sediment load. Second, the rainfall-reservoir composite index (RRCI) combining a rainfall index and a reservoir index is introduced, and the modified RRCI (denoted as $RRCI^S$) for the attribution of sediment load change is defined. Then, a rainfall-augmented sediment trapping index (RSTI) is developed by coupling the effective rainfall with the reservoir sediment trapping capacity. Finally, eight different linear or nonlinear regression models are established to simulate sediment load. The methods used in this study are described in detail in the following subsections.

3.1 Trend and change-point analysis

3.1.1 Mann-Kendall test

The Mann-Kendall (MK) test has been widely used in the trend analysis of hydro-meteorological series such as flow and rainfall as a typical non-parametric method recommended by the World Meteorological Organization (Mann, 1945; Kendall, 1975), which is conducive to the preliminary identification of characteristics of hydrological series.

For a series $x_1, x_2, ..., x_n$ that satisfies the independent identically distributed condition and as the number of observations becomes large, the Mann-Kendall statistic S is defined as follows:

$$S = \sum_{i=2}^{n} \sum_{j=1}^{i-1} \mathrm{sign}(x_i - x_j) \tag{1}$$

where

$$\mathrm{sign}(x_i - x_j) = \begin{cases} 1 & x_i > x_j \\ 0 & x_i = x_j \\ -1 & x_i < x_j \end{cases} \tag{2}$$

The variance of S is $Var(S) = \frac{n(n-1)(2n+5)}{18}$, and the standard normal statistic Z is calculated as follows:

$$Z = \begin{cases} (S-1)/\sqrt{Var(S)} & S > 0 \\ 0 & S = 0 \\ (S+1)/\sqrt{Var(S)} & S < 0 \end{cases} \tag{3}$$

The significance of trend can be tested by comparing Z with the standard normal variate at the significance level α (α=0.05 in this paper). The series has an upward trend when $S > 0$, while $S < 0$ indicates that it has a downward trend.

3.1.2 Pettitt test

The Pettitt (PT) test has been commonly used in the change-point detection of continuous hydro-meteorological series as a non-parametric test method proposed by Pettitt (Pettitt, 1979).

For a series $x_1, x_2, ..., x_n$ with n observations, the Pettitt statistic K_t is defined as:

$$K_t = \max |U_{t,n}| \tag{4}$$

in which,

$$U_{t,n} = \sum_{i=1}^{t} \sum_{j=t+1}^{n} \mathrm{sign}(x_i - x_j) \quad (t=1,2,\ldots,n) \tag{5}$$

where, $\mathrm{sign}(\cdot)$ is the sign function the same as the Equation (2). The change-point of the series is located at K_t, at the same time, Equation (6) is used to calculate the probability values (p_{PT}). If the p_{PT} is less than 0.05, the change-point is significant.

$$p_{\mathrm{PT}} = 2\exp\left(\frac{-6K_t^2}{n^3 + n^2}\right) \tag{6}$$

3.2 Rainfall-reservoir composite index (RRCI)

Xiong *et al*. (2019) developed the rainfall-reservoir composite index (RRCI) to assess the impacts of reservoirs on downstream flood frequency by coupling the effect of scheduling-related multivariate rainfall. The multiday antecedent rainfall input (MARI) is a critical event to form the downstream extreme flow. Five variables were used to describe the MARI for determining the peak, the total volume, the peak appearance time of inflow: the maximum daily rainfall, the mean daily rainfall, the total daily rainfall, the end time of MARI during that year, and the distance between the rainfall center and the outlet. The RRCI was derived from combining the reservoir index (RI) and a rainfall index. It is defined as follows:

$$\mathrm{RRCI} = \begin{cases} \left(P_{\mathrm{MARI}}^{\vee} \left(\bigcup_{i=1}^{d} (X_i > x_i) \right) \right)^{\frac{1}{\mathrm{RI}} - 1}, & 0 < \mathrm{RI} \le 1 \\ \mathrm{RI}, & \mathrm{RI} > 1 \end{cases} \tag{7a}$$

where, $P_{\mathrm{MARI}}^{\vee}$ is the OR joint exceedance probability that any one of the scheduling-related MARI variables (denoted as $X_1, X_2, ..., X_d$) will be exceeded and it acts as a rainfall index here. $P_{\mathrm{MARI}}^{\vee}$ is calculated by cumulative distribution function ($F(x_1, x_2, ..., x_d)$) that determines the dependence relationship of MARI variables, namely

$$P^{\vee}_{\mathrm{MARI}}\left(\bigcup_{i=1}^{d}(X_i > x_i)\right) = 1 - F(x_1, x_2, ..., x_d) \tag{7b}$$

And a dimensionless indicator—reservoir index (RI) (López and Francés, 2013) reflecting the impact of reservoirs on hydrological series in river basin is expressed as

$$\mathrm{RI} = \sum_{i=1}^{N}\left(\frac{A_i}{A_T}\right)\cdot\left(\frac{V_i}{\bar{Q}}\right) \tag{8}$$

where N is the total number of reservoirs upstream of the certain hydrological station; A_i is the catchment area controlled by the i-th reservoir upstream, km^2; A_T is the total catchment area controlled by the hydrological station, km^2; V_i is the total storage capability of the i-th reservoir upstream, m^3; and $\bar{Q}$ is the mean annual runoff at the hydrological station, m^3. The RI is generally less than 1 for a reservoir system consisting of small- and middle-sized reservoirs, while it may be close to or greater than 1 for a reservoir system with some large reservoirs like multi-year regulating storage reservoirs.

In this study, a modification is made to Equation (7). Effective rainfall is used to replace the multiday antecedent rainfall input (MARI) to measure the impact of rainfall on sediment load rather than on floods.

$$\mathrm{RRCI}^S = \begin{cases} 0, & \mathrm{RI} = 0 \\ (1 - F_n)^{\frac{1}{\mathrm{RI}} - 1}, & 0 < \mathrm{RI} \le 1 \\ \mathrm{RI}, & \mathrm{RI} > 1 \end{cases} \tag{9}$$

where, F_n is the empirical cumulative distribution function of the dependence relationship of effective rainfall amount and rainfall intensity introduced in Section 3.3.1.

3.3 Construction of rainfall-augmented sediment trapping index (RSTI)

RRCI is constructed for measuring the effects of antecedent rainfall and reservoir storage capacity on the downstream flood regime. The capture of rainfall information and the consideration of reservoir effects in RRCI are no longer applicable to the study of sediment. Therefore, in this subsection, a rainfall-augmented sediment trapping index (RSTI) is derived from combining effective rainfall information (including effective rainfall amount and rainfall intensity) and reservoir sediment trapping capacity (reflected by the indicator TE, i.e. sediment trapping efficiency of reservoirs) for attributing the downstream sediment load change. The specific procedures will be described in detail below.

3.3.1 Effective rainfall

Rainfall has a great impact on sediment load (Berger *et al*., 2010), and it is the most important power factor in causing soil erosion; however, not all rainfall events can produce floods and then lead to soil erosion, only rainfall causing the generation of substantial runoff or floods can initiate and transport sediment (i.e. erosive rainfall that forms sediment) (Xie *et al*., 2002). Rainfall amount (denoted as A) and rainfall intensity (denoted as I), as the main characteristics of rainfall, are highly correlated with soil loss (Lal, 1976; Pruski and Nearing, 2002; Wu *et al*., 2018a). Therefore, sediment yield is affected by both rainfall amount and rainfall intensity. In order to identify the most effective rainfall events affecting sediment generation and transport in terms of both amount and intensity, different threshold levels of rainfall intensity (mm/day) are set to calculate corresponding effective rainfall amount (mm) and effective rainfall intensity (mm/day) for each year. In this study, 14 threshold levels (TL) for daily rainfall intensity, i.e. TL= 2, 4, 6, 8, 10, 15, 20, 25, 30, 35, 40, 45, 50, or 55 mm/day, are first selected. Then, for each year from 1952 to 2017, the annual effective rainfall amount for each given TL is calculated by summing the amount of all daily rainfall events with an intensity higher than the given TL value and denoted by A_2, A_4, A_6, A_8, A_{10}, A_{15}, A_{20}, A_{25}, A_{30}, A_{35}, A_{40}, A_{45}, A_{50} and A_{55}, respectively. Next, for each year, the annual effective rainfall intensity for each given TL is calculated by averaging all daily rainfall intensity with an intensity higher than the given TL value and denoted by I_2, I_4, I_6, I_8, I_{10}, I_{15}, I_{20}, I_{25}, I_{30}, I_{35}, I_{40}, I_{45}, I_{50} and I_{55}, respectively. In determining a criterion for defining effective rainfall events and calculating annual effective rainfall amount, the optimum threshold level of daily rainfall intensity is chosen to be the TL value that makes the Pearson correlation coefficient between annual sediment load and annual effective rainfall amount maximum. Similarly, in determining a criterion for calculating annual effective rainfall intensity, the optimum threshold level of daily rainfall intensity is set to be the TL value that makes the Pearson correlation coefficient between annual sediment load and annual effective rainfall intensity maximum.

The joint non-exceedance probability acts as a rainfall index capturing effective rainfall information to measure the rainfall effects on sediment, and it is the probability that neither rainfall amount nor rainfall intensity exceeds. The higher this probability is, the greater the rainfall effects on sediment. The relationship between joint distribution function of rainfall amount and rainfall intensity ($F(a,i)$) and non-exceedance probability ($P(A \le a,\ I \le i)$) is expressed as follows:

$$F(a,i) = P\{(A \le a) \cap (I \le i) = P(A \le a,\ I \le i) \tag{10}$$

In order to increase applicability of rainfall index and related indicators in practice, the empirical copula is used to calculate joint distribution function in this study.

$$F_n(a_i, i_i) = \frac{1}{n}\sum_{i=1}^{n} 1\{\hat{A} \le a_i, \hat{I} \le i_i\} \tag{11}$$

where, $F_n(a_i, i_i)$ is the empirical distribution function of the dependence relationship of A and I; $\hat{A}$ and $\hat{I}$ denote the pseudo-observations of effective rainfall amount and rainfall intensity, respectively; n is the sample size.

3.3.2 Sediment trapping efficiency (TE) of reservoirs

Sediment trapping efficiency (TE) of reservoirs originally proposed by Brune (1953) is expressed as a function of residence time ($\Delta\tau$) to predict a single reservoir trapping efficiency.

$$\mathrm{TE}_{\mathrm{single}} = 1 - \frac{0.05}{\sqrt{\Delta\tau_{\mathrm{single}}}} \tag{12a}$$

$$\Delta\tau_{\mathrm{single}} = \frac{V}{\bar{Q}} \tag{12b}$$

Vörösmarty *et al*. (2003) developed a method for basin-wide sediment trapping efficiency calculations, which is defined as

$$\mathrm{TE}_{\mathrm{basin}} = 1 - \frac{0.05}{\sqrt{\Delta\tau_{\mathrm{basin}}}} \tag{13a}$$

$$\Delta\tau_{\mathrm{basin}} = \frac{\sum_{i=1}^{N} V_i}{\bar{Q}} \tag{13b}$$

Considering the differences in geographical location within the catchment, physical characteristics and operation strategy of the reservoir, the Brune model is suggested to be modified by adding a correction coefficient α (Fu and He, 2007; Kummu *et al*., 2010; Li *et al*., 2020), thus becoming.

$$\mathrm{TE}^{*}_{\mathrm{basin}} = 1 - \frac{0.05\alpha}{\sqrt{\Delta\tau_{\mathrm{basin}}}} \tag{14a}$$

In this paper, the correction coefficient α is proposed to be calculated by the following formula.

$$\alpha = \frac{A_T}{A_L} \tag{14b}$$

where A_L is the largest upstream control area of all the reservoirs built in the basin, km^2; and the other symbols have the same meaning as Section 3.2. The influence of reservoir's geographical location within the total catchment on TE is reflected by α; and α is kept 1 when there is only one reservoir in the basin.

3.3.3 Rainfall-augmented sediment trapping index (RSTI)

In order to assess comprehensively the impacts of effective rainfall and sediment trapping capacity of the reservoirs on sediment load, the rainfall-augmented sediment trapping index (RSTI) for a downstream gauging station is defined in a similar way to RRCI as shown in Section 3.2 (Xiong *et al.*, 2019).

$$\mathrm{RSTI} = \begin{cases} 0, & \mathrm{TE} = 0 \\ (1 - F_n)^{\frac{1}{\mathrm{TE}} - 1}, & 0 < \mathrm{TE} \le 1 \end{cases} \tag{15}$$

where, F_n is the empirical distribution function computed by Equation (11); TE is the sediment trapping efficiency of the reservoirs in the basin calculated by Equation (14); the expectation of the RSTI is $\mathrm{E(RSTI)} = \mathrm{TE}$.

The relationships in Equation (9) and Equation (15) are illustrated in **Figure 2**, the shaded area of the left panel is the variation range of RI, and the shaded area of the right panel represents the range of TE in the Wujiang River.

< Figure 2>

3.4 Regression models for simulating sediment load

The regression method is widely used to carry out change attribution analysis of hydrological series by hydrologists, and it can directly reflect the relationship between the dependent variables and explanatory variables (Bezak *et al*., 2017; Jiang *et al*. 2011; Wang *et al*., 2017; Xu, 2009). The different linear or nonlinear regression models are constructed to simulate sediment load values in this subsection (**Table 3**). M1 and M2 separately take into account the effects of the three explanatory variables (i.e. the most effective rainfall amount, the most effective rainfall intensity and reservoir index) selected in this paper on sediment load change. M3 and M4 are constructed by combining effect of rainfall amount and rainfall intensity based on M1 and M2. M5-M8 use piecewise fitting method to simulate sediment load, only the impact of rainfall on sediment load is considered before 1984 (1984 is the year when the first large-scale reservoir—Wujiangdu Reservoir was put into full operation), RRCI^S and RSTI are used to assess the impacts of reservoirs on downstream sediment load by coupling the effect of effective rainfall after 1984. Linear regression (denoted as LR) in additive form (including: M1, M3, M5, M7) and nonlinear regression (denoted as NLR) in product form (including: M2, M4, M6, M8) are considered in the above models. Among them, NLR takes into account the interaction between different explanatory variables very conveniently, while it is difficult to add the correct interaction terms for LR and it usually takes a lot of time. At the same time, NLR model avoids the possible negative values of simulated sediment load compared with the LR model. The parameters in formulas (i.e. *a*, *b*, *c*, *d*) of all models are estimated by least-square estimation. The parameters of the NLR model are also estimated by least-square method, but the premise is variable transformation from nonlinear to linear model. The validity of the model and the significance of the model parameters are tested by *F* test and *t* test (Moore *et al.*, 2009) for the regression models.

< Table 3>

In order to evaluate the performance of eight regression models displayed in **Table 3**, correlation coefficient (*R*), Nash-Sutcliffe efficiency coefficient (NSE; Nash and Sutcliffe, 1970), and relative error (RE) are introduced as follows, respectively:

$$R = \frac{\sum_{t=1}^{n}(S_t^{obs} - \bar{S}^{obs})(S_t^{sim} - \bar{S}^{sim})}{\sqrt{\sum_{t=1}^{n}(S_t^{obs} - \bar{S}^{obs})^2 \cdot \sum_{t=1}^{n}(S_t^{sim} - \bar{S}^{sim})^2}} \tag{16a}$$

$$\text{NSE} = 1 - \frac{\sum_{t=1}^{n}(S_t^{obs} - S_t^{sim})^2}{\sum_{t=1}^{n}(S_t^{obs} - \bar{S}^{obs})^2} \tag{16b}$$

$$\text{RE} = \frac{\sum_{t=1}^{n}|S_t^{obs} - S_t^{sim}|}{\sum_{t=1}^{n}S_t^{obs}} \tag{16c}$$

where, S_t^{obs} is the observed sediment load in *t* year; S_t^{sim} is the simulated sediment load in year of *t*; $\bar{S}^{obs}$ and $\bar{S}^{sim}$ are the mean values of the observations and simulations.

4 Results

4.1 Temporal variation of hydrological series

The Mann-Kendall test and Pettitt test are used for trend and change-point testing of annual rainfall, annual runoff and annual sediment load of the WRB, the results are shown in **Table 4**. According to the results of the Mann-Kendall test, rainfall and runoff of the Wujiang River have no obvious changing trend, sediment load is characterized by strikingly decreasing trend during the period of 1952-2017 at the 5% significance level. The results of the Pettitt test show that there is a significant change-point in sediment load, and its corresponding mutation year is 1984 when the Wujiangdu Reservoir was put into full operation (the Wujiangdu Reservoir is the first large-scale reservoir on the main stream of the Wujiang River; it was built from 1970, began to store water in

1979, and was completed in 1983; in addition, at the beginning of the construction of Wujiangdu reservoir, the average annual sediment trapping was more than 20 million tons). Rainfall changes slightly in 1984, which is consistent with the mutation year of sediment load.

The inter-annual time series of rainfall, runoff and sediment load are displayed in **Figure 3**. It can be seen from the figure that sediment load presents a significant change and decreases obviously after 1984, while rainfall and runoff fluctuate steadily near the mean, which further confirms the results of Mann-Kendall test and Pettitt test. The mean annual rainfall is 1137 mm, and the mean annual runoff of the WRB is 487×10^8 m^3 during 1952-2017. Comparing the mean values of sediment load before and after the change-point, it plummets from 3299×10^4 t/a (during 1952-1983) to 1267×10^4 t/a (during 1984-2017), reducing by 62%.

< Table 4>

< Figure 3>

4.2 Rainfall and reservoir effects on sediment load change

4.2.1 Identification of the most effective rainfall

Table 5 displays the Pearson linear correlation between annual rainfall characteristics (including rainfall amount and rainfall intensity with 14 threshold levels as described in Section 3.3.1) and annual sediment load. It was found that, A_6 and I_2 are the most relevant rainfall characteristics for sediment load. Therefore, A_6 and I_2 are selected as the most effective rainfall explanatory variables to simulate sediment load. When the threshold level of rainfall intensity is chosen to be greater than or equal to 30 mm/day, there are zero values in the time series of both annual effective rainfall amount and annual effective rainfall intensity, which lead to a poor correlation between rainfall characteristics and sediment load.

< Table 5>

4.2.2 Correlation between sediment load and explanatory variables

The joint distribution function (F_n) is computed by substituting A_6 and I_2 into Equation (11). Then, RRCI^S and RSTI are calculated based on the calculation of RI and TE, respectively. As shown in **Figure 4**, all explanatory variables (including: A_6, I_2, RI, F_n, RRCI^S, RSTI) are significantly correlated with sediment load (S). Among which, A_6, I_2 and F_n are positively correlated with S; RI, RRCI^S and RSTI have negative correlation with S, which is reasonable. RSTI has the strongest correlation with sediment load because it integrates the effects of rainfall and sediment trapping by reservoirs on S. By the way, the times series of all explanatory variables are presented in

Figure 4. The fluctuations of A_6, I_2 and F_n are stable, and there is no obvious trend. While, RI increases year by year with the construction of reservoirs; $RRCI^S$ and RSTI are increasing dynamically due to the combination of rainfall and reservoir impacts.

< Figure 4>

4.3 Simulating sediment load by regression models

M1-M8 presented in Section 3.4 are constructed based on the regression method, the testing results of the validity of models (*F* test) and the significance of model parameters (*t* test) are displayed in **Table 6**. It was found that all models passed the *F* test, and parameters of all models passed the *t* test except for M1 and M2. The Pearson correlation coefficient of A_6 and I_2 is 0.704, correlation coefficient between A_6 and RI is -0.186, and that between I_2 and RI is -0.025. Condition indices (Midi *et al*., 2010) corresponding to three and four dimensions are 16.001 and 36.663 for M1, 63.529 and 132.564 for M2, which are beyond the range of rule of thumb (i.e. 15) and indicate a serious collinearity problem. The existence of collinearity can cause inaccurate or unstable estimates of models (Midi *et al*., 2010). In order to overcome the collinearity problem, we drop I_2 from the covariates in M1 and M2 based on the fact that the correlation between A_6 and sediment load is stronger than that between I_2 and sediment load.

< Table 6>

After dropping the covariate I_2, improved models $M1^*$ and $M2^*$ are set up to replace M1 and M2. The formulas of $M1^*$ and $M2^*$ are as follows:

$$\mathrm{M1}^*:\quad S^{sim} = a + b \cdot A_6 + c \cdot \mathrm{RI} \tag{17}$$

$$\mathrm{M2}^*:\quad S^{sim} = a \cdot (A_6)^b \cdot (1 - \mathrm{RI})^c \tag{18}$$

Both $M1^*$ and $M2^*$ passed the test of the validity of models (*F* test) and the significance of model parameters (*t* test). The co-existence of rainfall amount and rainfall intensity will lead to the multicollinearity, but removing rainfall intensity will lose part of the rainfall information, so coupling them is particularly necessary. Compared with independent consideration of the impacts of A_6 and I_2 on sediment load change, the joint distribution of A_6 and I_2 can not only solve the collinearity problem of the model without losing rainfall information, but also improve the simulation effect of the model. The comparison between $M2^*$ and M4 indicated that the simulation considering the combined effect of rainfall amount and rainfall intensity is better than rainfall amount alone (**Figure 5**). Simulated sediment load of eight regression models is displayed in **Figure 5**. According to the results of model evaluation indicators (i.e. *R*, NSE, RE), eight regression models can both simulate sediment load well, and the model with the best simulation effect corresponding to M8. Compared with the linear regression (LR) model ($M1^*$, M3, M5, M7), the nonlinear regression model (NLR) with the same covariates ($M2^*$, M4, M6, M8) has better performance. The LR model is not reasonable because there are negative values (or abnormal values) in the simulated sediment load, it can be seen from the crosses in $M1^*$, M3, M5 of **Figure 5**. The performance of M8 is better than M4, which demonstrates that rainfall-augmented sediment trapping index (RSTI) coupling the effective rainfall with the reservoir sediment trapping capacity could better explain the change of sediment load than separate consideration of rainfall and reservoir impacts. And the performance of M8 is better than M6, which indicates that the explanatory power of RSTI proposed in this paper is greater than rainfall-reservoir composite index ($RRCI^S$) coupling the effective rainfall with the reservoir index in the simulation of observed sediment load series. The reason for the poor results about $RRCI^S$ is that reservoir regulation on sediment load is underestimated under heavy rainfall and overestimated under weak rainfall (**Figure 2**). For all models, M8 has the smallest variation range of residual (the difference between observed and simulated sediment load, namely ΔS), followed by M4 (**Figure 6)**.

< Figure 5>

< Figure 6>

5 Discussions

5.1 Effects of rainfall and reservoir on the sediment load

Rainfall is a critical factor in sediment formation (Donjadee and Chinnarasri, 2012; Ran *et al*., 2012), rainfall information such as rainfall amount and rainfall intensity directly affects soil loss intensity, and the intensity of soil loss is closely related to rainfall alteration (Pruski and Nearing, 2002; Lu *et al*., 2013). Because of the continuous rainfall process, even a small rainfall in humid areas (the Wujiang River Basin is a humid area) will cause sediment generation on the slope (Ziadat and Taimeh, 2013), the effective rainfall amount (A_6, rainfall amount with an intensity higher than 6 mm/day) and rainfall intensity (I_2, rainfall intensity higher than 2 mm/day) selected in Section 4.2.1 conform to the rule.

Sediment trapping by reservoirs is the leading driving factor to the reduction of sediment load in rivers (Li *et al*., 2016; Wu *et al*., 2018b; Xu, 2009), for example, the dam constructions in the Yangtze River have a significant impact on the variation of the sediment in the basin (Li *et al*., 2011). Sediment load in the Wujiang River Basin changed dramatically in 1984, which corresponds to the full operation of the first large-scale reservoir on the main stream of the basin (i.e. Wujiangdu Reservoir). With the increase of the number of reservoirs in the basin (or the increase of the total storage capacity of reservoirs), the sediment load continues to decrease (**Figure 3**). This is consistent with previous studies about the impact of reservoirs on the reduction of sediment load in the Wujiang River (Wu *et al*., 2018b).

In Section 4.3, the performance of M8, i.e. Equations (19a) and (19b), was significantly better than that of the other seven models, thus M8 is selected to investigate the influences of rainfall erosion and reservoir interception on sediment load, as shown in **Figure 7**. In **Figure 7**, the simulated sediment load of model M8 is represented by the dotted red line, in which the simulation of sediment load was only related to effective rainfall for the period of 1952-1983 when there wasn't any reservoirs built as shown by Equation (19a), and for the period of 1984-2017 the simulation of sediment load was affected by both rainfall and reservoir as shown by Equation (19b). The simulated sediment load of M8 is close to the observed sediment load (solid blue line) for the total period of 1952-2017. In **Figure 7**, the dotted black line for the period of 1984-2017 is the simulated sediment load computed by Equation (20), which is just an extension of Equation (19a) from period of 1952-1983 to the period of 1984-2017, and represents the sediment load caused by only rainfall under the assumption of no reservoirs, which means that the actual interception of reservoir on sediment load is not taken into account. Therefore, for the period of 1984-2017, the simulated sediment load calculated by Equation (20) will be larger than that computed by Equation (19b), and the difference between the dotted black line from Equation (20) and the dotted red line from Equation (19b) is assumed to be the sediment load intercepted by reservoirs and displayed as gray columns in **Figure 7**. From the height of the gray columns in **Figure 7**, we can observe that with the increase of the number of reservoirs in the basin, the amount of sediment load intercepted by the reservoirs gradually increases. In addition, the sediment load intercepted by reservoirs based on M8 (marked as *SM*) gets close to estimated sediment load from reservoir interception (marked as *ES*) in most years, as displayed in **Figure 8**. Where *ES* is obtained by superposition calculation according to the data of sediment trapping by all reservoirs in **Table 1**. This further indicates that the sediment load simulated by model M8 is close to the observations. Rainfall erosion increases sediment load, and reservoir interception reduces sediment load, the combined effect of the two can better explain the change of the total sediment load in the Wujiang River Basin. Therefore, the RSTI constructed in this paper considering the coupled impact of rainfall and reservoir on sediment load might be a useful index for evaluating the effects of rainfall and reservoir on sediment load.

$$S^{sim} = \begin{cases} 4670.0 \cdot F_n^{\,0.4}, & 1952 \le t \le 1983 \quad (19a) \\ 2828.4 \cdot (1 - \mathrm{RSTI})^{0.6}, & 1984 \le t \le 2017 \quad (19b) \end{cases}$$

$$S^{sim} = 4670.0 \cdot F_n^{\,0.4},\ 1952 \le t \le 2017 \quad (20)$$

< Figure 7>

Compared with the mean value of sediment load from 1952 to 1983 (3299×10^4 t), the reduction of observed sediment load (marked as *RS*) during the period of 1984-2017 (the period after the change point 1984) is shown in **Figure 8**. The values of *RS* (blue column) and *ES* (red column) are very close in most years, which demonstrates that the effect of reservoirs on sediment load is dominant. The abnormal changes of sediment load in certain years (e.g., 1996, 1998) may have been related to rainfall or flood of that year to a large extent (the peak discharge is 20000 m^3/s in 1996 and 13100 m^3/s in 1998 at Wulong station of the Wujiang River).

< Figure 8>

Finally, the estimation errors of the sediment trapping by reservoirs should be noted. Except for the impact of climate change including rainfall on sediment load, the differences between *RS* and *ES* are mainly due to the following reasons: (1) the lack of consideration that the capacity of sediment trapping by reservoirs decreases with the increase of reservoir construction years; (2) the change of underlying surface conditions, such as land cover and land use patterns change; (3) sand mining activities, and so on.

5.2 Contribution of underlying surface conditions to sediment load change

Change in underlying surface condition caused by human activities is another crucial factor directly affects the process of sediment yield (Xu *et al*., 2018; Zhang *et al*., 2018). Next, the impact of underlying surface condition on sediment load is analyzed based on the available data.

The time series of normalized difference vegetation index (NDVI) is shown in **Figure 9**. NDVI changes steadily from 0.55 to 0.65 during 1982-2015, which indicates that the vegetation coverage of the WRB has not changed significantly.

< Figure 9>

Land-use and land-cover change (LUCC) of the Wujiang River in 1980 and 1990 is compared in **Figure 10**, it has no distinct change from 1980 to 1990. The area and percentage of every land use patterns are shown in **Table 7** by statistical calculation. The area of vegetation coverage (including forestland and grassland) occupied 69% in 1980 and 68% in 1990 of basin area, it decreased by 595 km^2, and urban land areas increased by 43 km^2. Cropland

and unused land areas increased by 561 km^2 and 4 km^2, respectively, and the area of water body decreased by 13 km^2. The weak change of LUCC suggests that it has no significant effect on abrupt change (1984) of sediment load in the WRB. In the 1980s, the Chinese government began to pay attention to the problem of soil erosion and water conservation, but the work of returning farmland to forest or grassland was slow, and a large number of steep slopes above 25 degrees were still under cultivation in the WRB (Wu *et al*., 2018c).

< Figure 10>

< Table 7>

To sum up, it can be inferred that vegetation cover and land use patterns have no significant impacts on sediment load change in the Wujiang River. This result needs to be verified in more other river basins, and historical data should be collected extensively to lengthen the time series of underlying surface so as to make the result more reliable.

6 Conclusions

In this study, a rainfall-augmented sediment trapping index (RSTI) was developed to evaluate the coupled effect of rainfall and reservoirs on downstream sediment load of the Wujiang River. Then, eight models were set up to investigate how to best utilize the RSTI to simulate the observed sediment load based on the linear and nonlinear regression methods. The primary conclusions are as follows.

(1) The sediment load in the Wujiang River is characterized by a decreasing trend and a significant abrupt change in 1984 when the Wujiangdu Reservoir (the first large-scale reservoir on the main stream of the Wujiang River Basin) was put into full operation, and the mutation year 1984 also corresponds to the year of rainfall abruption.

(2) Both the linear regression model and the nonlinear regression model with RSTI as the covariate are superior to the cases with other factors as the covariate. And the most effective rainfall characteristics are A_6 (i.e. rainfall amount with an intensity higher than 6 mm/day) and I_2 (i.e. rainfall intensity higher than 2 mm/day) for developing RSTI.

(3) According to the comparison of simulated sediment load of eight regression models, nonlinear regression can better illustrate the effects of rainfall and reservoirs on sediment load. The nonlinear regression model with RSTI (i.e. rainfall-augmented sediment trapping index, which couples the impacts of effective rainfall and sediment trapping capacity of reservoirs) as a covariate can best simulate the sediment load, this indicates that RSTI can more completely capture the non-stationarity of the downstream sediment load.

Therefore, in this study, we identified the impacts of rainfall erosion and reservoir interception on sediment load change and provided a satisfactory quantitative relationship between rainfall, reservoir and sediment load for downstream sediment management under a changing environment.

Acknowledgements

This research is financially supported jointly by the National Natural Science Foundation of China (NSFC Grants 41890822 and 51525902), the Research Council of Norway (FRINATEK Project 274310), and the Ministry of Education "Plan 111" Fund of China (B18037), all of which are greatly appreciated. No conflict of interest exists in the submission of the manuscript.

References

Berger, C., Schulze, M., Rieke-Zapp, D., Schlunegger, F., 2010. Rill development and soil erosion: a laboratory study of slope and rainfall intensity. Earth Surf. Proc. Land., 35(12), 1456-1467.

Bezak, N., Rusjan, S., Fijavž, M.K., Mikoš, M., Šraj, M., 2017. Estimation of Suspended Sediment Loads Using Copula Functions. Water, 9(8), 628.

Brune, G. M., 1953. Trap efficiency of reservoirs. Eos Transactions American Geophysical Union, 34(3), 407-418.

Carriquiry, J.D., Sanchez, A., 1999. Sedimentation in the Colorado River delta and Upper Gulf of California after nearly a century of discharge loss. Mar. Geol., 158, 125-145.

Chen, C., Xu, Q., Chen, Z., 2008. Analysis on variation characteristics and influencing factors of runoff and sediment in the Wujiang River basin. J. Sediment Res., 5, 43-48. (In Chinese)

Donjadee, S., Chinnarasri, C., 2012. Effects of rainfall intensity and slope gradient on the application of vetiver grass mulch in soil and water conservation. Int. J. Sediment Res., 27(2), 168-177.

Fu, K., He, D., 2007. Analysis and prediction of sediment trapping efficiencies of the reservoirs in the mainstream of the Lancang River. Chinese Sci. Bull., 52(supp. II), 134-140.

Huang, S., Li, P., Huang, Q., & Leng, G., 2017. Copula-based identification of the non-stationarity of the relation between runoff and sediment load. Int. J. Sediment. Res., 32(2), 221-230.

Jiang, S., Ren, L., Yong, B., Singh, V. P., Yang, X., Yuan, F., 2011. Quantifying the effects of climate variability and human activities on runoff from the Laohahe Basin in northern China using three different methods. Hydrol. Process., 25 (16), 2492-2505.

Kendall, M. G., 1975. Rank correlation methods. Charles Griffin, London.

Kummu, M., Lu, X., Wang, J., Varis, O., 2010. Basin-wide sediment trapping efficiency of emerging reservoirs along the Mekong. Geomorphology, 119(3-4), 181-197.

Lal, R., 1976. Soil erosion on alfisols in western Nigeria: Ⅲ. Effects of rainfall characteristics. Geoderma, 16(5), 389-401.

Lal, R., 1994. Soil erosion by wind and water: problems and prospects, in: Lal, R. (Ed.), Soil erosion research methods, 2nd Edition. Soil and Water Conservation Society, St. Lucie Press, New York, pp. 1-9.

Li, H., Huang, D., Xu, C., Liang R., 2020. Processes of sediment transport in the Xijiang River. J. Sediment Res., 45(1), 52-58. (In Chinese)

Li, N., Wang, L., Zeng, C., Wang, D., Liu, D., Wu, X., 2016. Variations of Runoff and Sediment Load in the Middle and Lower Reaches of the Yangtze River, China (1950-2013). Plos One, 11(8), e0160154.

Li, Q., Yu, M., Lu, G., Cai, T., Bai, X., Xia, Z., 2011. Impacts of the Gezhouba and Three Gorges reservoirs on the sediment regime in the Yangtze River, China. J. Hydrol., 403(3-4), 224-233.

López, J., Francés, F., 2013. Non-stationary flood frequency analysis in continental Spanish rivers, using climate and reservoir indices as external covariates. Hydrol. Earth Syst. Sc., 17(8), 3189-3203.

Lu, X., Ran, L., Liu, S., Jiang, T., Zhang, S., Wang, J., 2013. Sediment loads response to climate change: A preliminary study of eight large Chinese rivers. Int. J. Sediment. Res., 28(1), 1-14.

Mann, H. B., 1945. Nonparametric tests against trend. Econometrica, 13, 245-259.

Miao, C. Y., Borthwick, N. J. R., Yang, A. G. L., 2011. A preliminary estimate of human and natural contributions to the changes in water discharge and sediment load in the Yellow River. Global Planet. Change, 76(3-4), 196-205.

Midi, H., Sarkar, S.k., Rana, S., 2010. Collinearity diagnostics of binary logistic regression model. J. Interdiscipl. Math., 13(3), 253-267.

Moore, D. S., McCabe, G. P., Craig, B. A., 2009. Introduction to the practice of statistics (Sixth edition). W. H. Freeman and Company, New York.

Nash, J. E., Sutcliffe, J., 1970. River flow forecasting through conceptual models, Part 1: A discussion of principles. J. Hydrol., 10, 282-290.

Pelletier, J. D., 2012. A spatially distributed model for the long-term suspended sediment discharge and delivery ratio of drainage basins. J. Geophys. Res., 117, F02028.

Peng, J., Chen, S., Dong, P., 2010. Temporal variation of sediment load in the Yellow River basin, China, and its impacts on the lower reaches and the river delta. Catena, 83(2-3), 135-147.

Pettitt, A. N., 1979. A non-parametric approach to the change point problem. J. R. Stat. Soc. C-Appl., 28, 126-135.

Pruski, F. F., Nearing, M. A., 2002. Runoff and soil-loss responses to changes in precipitation: A computer simulation study. J. Soil Water Conserv., 57(1), 7-15.

Ran, Q., Su, D., Li, P., He, Z., 2012. Experimental study of the impact of rainfall characteristics on runoff generation and soil erosion. J. Hydrol., 424–425(6), 99-111.

Rossi, A., Massei, N., Laignel, B., Sebag, D., Copard, Y., 2009. The response of the Mississippi River to climate fluctuations and reservoir construction as indicated by wavelet analysis of streamflow and suspended-sediment load, 1950-1975. J. Hydrol., 377, 237-244.

Singh, V. P., 1995. Environmental Hydrology. Springer, New York.

Syvitski, J. P. M., Milliman, J. D., 2007. Geology, geography, and humans battle for dominance over the delivery of fluvial sediment to the coastal ocean. J. Geol., 115(1), 1-19.

Uca, Ekhwan, T., Othman, J., Rosmini, M., Amal, A., Saleh, A. A., 2018. Daily suspended sediment discharge prediction using multiple linear regression and artificial neural network. J. Phys: Conf. Series, 954, 012030.

Vörösmarty, C. J., Meybeck, M., Fekete, B., Sharma, K., Green, P., Syvitski, J. P. M., 2003. Anthropogenic sediment retention: major global impact from registered river impoundments. Global Planet. Change, 39, 169-190.

Walling, D. E., 2006. Human impact on land-ocean sediment transfer by the world's rivers. Geomorphology, 79(3-4), 192-216.

Wang, Y., Hou, L., Cai, Y., 2017. Scale effects of eroded sediment transport in Wujiang River Basin, Guizhou Province, China. J. Groundwater Sci. Eng., 5(2), 182-192.

Wen, T., Xiong, L., Jiang, C., Hu, J., Liu, Z., 2019. Effects of climate variability and human activities on suspended sediment load in the Ganjiang River Basin, China. J. Hydrol. Eng., 24(11), 05019029.

Wiegel, R. L., 1996. Nile delta erosion. Science, 272, 338-340.

Wu, X., Wei, Y., Wang, J., Xia, J., Cai, C., Wei, Z., 2018a. Effects of soil type and rainfall intensity on sheet erosion processes and sediment characteristics along the climatic gradient in central-south China. Sci. Total Environ., 621, 54-66.

Wu, X., Xiang, X., Chen, X., Zhang, X., Hua, W., 2018b. Effects of cascade reservoir dams on the streamflow and sediment transport in the Wujiang River basin of the Yangtze River, China. Inland Waters, 8(2), 216-228.

Wu, X., Zhang, X., Xiang, X., Chen, X., Wang, C., Li, X., 2018c. Runoff and sediment variations in the upstream of Wujiang River Basin and the influences of hydropower station construction. Chinese J. Ecol., 37(3), 642-650. (In Chinese)

Xie, Y., Liu, B., Nearing, M. A., 2002. Practical thresholds for separating erosive and non-erosive storms. T. ASABE, 45(6), 1843-1847.

Xiong, B., Xiong, L., Xia, J., Xu, C., Jiang, C., Du, T., 2019. Assessing the impacts of reservoirs on downstream flood frequency by coupling the effect of scheduling-related multivariate rainfall with an indicator of reservoir effects. Hydrol. Earth Syst. Sc., 23, 4453-4470.

Xu, G., Zhang, J., Li, P., Li, Z., Lu, K., Wang, X., et al., 2018. Vegetation restoration projects and their influence on runoff and sediment in China. Ecol. Indic., 95, 233-241.

Xu, J., 2003. Sediment flux to the sea as influenced by changing human activities and precipitation: Example of the Yellow River, China. Environ. Manage., 31 (3), 328-341.

Xu, J., 2007. Trends in suspended sediment grain size in the upper Yangtze River and its tributaries, as influenced by human activities. Hydrolog. Sci. J., 52(4), 777-792.

Xu, J., 2009. Plausible causes of temporal variation in suspended sediment concentration in the upper Changjiang River and major tributaries during the second half of the 20th century. Quatern. Int., 208, 85-92.

Yang, S., Zhao, Q., Belkin IM, 2002. Temporal variation in the sediment load of the Yangtze River and the influences of human activities. J. Hydrol., 263, 56-71.

Yang, Z., Wang, H., Saito, Y., Milliman, J. D., Xu, K., Qiao, S., et al., 2006. Dam impacts on the Changjiang (Yangtze) River sediment discharge to the sea: The past 55 years and after the Three Gorges Dam. Water Resour. Res., 42, W04407.

Ziadat, F. M., Taimeh, A. Y., 2013. Effect of rainfall intensity, slope, land use and antecedent soil moisture on soil erosion in an arid environment. Land Degrad. Dev., 24(6), 582-590.

Zhang, X., Lin, P., Chen, H., Yan, R., Zhang, J., Yu, Y., et al., 2018. Understanding land use/cover change impacts on runoff and sediment load at flood events on the Loess Plateau, China. Hydrol. Process., 32, 576-589.

Zhu, Y., Lu, X., Zhou, Y., 2008. Sediment flux sensitivity to climate change: A case study in the Longchuanjiang catchment of the upper Yangtze River, China. Global Planet. Change, 60(3), 429-442.

Tables

Table 1 Information of the reservoirs in the Wujiang River Basin

Reservoir	Longitude (E)	Latitude (N)	Catchment area (km^2)	Total capacity (10^8 m^3)	Sediment trapping (10^4 t/year)	Completion year
Yinpan	107.89	29.28	74910	3.20	6.6	2011
Pengshui	108.20	29.20	69000	14.65	460.0	2009
Shatuo	108.47	28.50	54508	9.10	97.3	2012
Silin	108.19	27.80	48558	15.93	97.5	2005
Goupitan	107.63	27.38	43250	64.54	273.0	2004
Wujiangdu	106.76	27.32	27790	23.00	2180.0(1984-1990) 1500.0(1991-1993) 13.0(1994-2015)	1983
Suofengying	106.37	26.97	21862	2.01	0.008	2005
Dongfeng	106.16	26.86	18161	10.25	1320.0(1994-2005) 528.0(2006-2015)	1994
Yinzidu	106.14	26.58	6422	5.29	327.7	2002
Hongjiadu	105.85	26.87	9900	49.47	600.0	2004
Puding	105.81	26.38	5871	3.99	250.0	1995

Table 2 Mean annual rainfall data of 15 meteorological stations in the Wujiang River Basin during the period of 1952-2017.

Meteorological station	Altitude (m a.s.l.)	Longitude (E)	Latitude (N)	Mean annual rainfall (mm)
Lichuan	1074.1	108.56	30.17	1296
Enshi	457.1	109.28	30.17	1437
Fengdu	290.5	107.44	29.51	1052
Qianjiang	607.3	108.47	29.32	1189
Zhengan	679.7	107.27	28.33	1060
Youyang	826.5	108.46	28.49	1354
Bijie	1510.6	105.17	27.18	907
Renhuai	890.3	106.24	27.48	1006
Xifeng	1038.1	106.43	27.06	1119
Meitan	792.2	107.28	27.46	1118
Yuqing	622.1	107.53	27.14	1075
Sinan	416.8	108.15	27.57	1130
Qianxi	1231.4	106.01	27.02	962
Zhijin	1319.3	105.46	26.41	1381
Guiyang	1223.8	106.44	26.35	1119

Table 3 Eight different linear or nonlinear regression models for simulation of the sediment load in the Wujiang River Basin during the period of 1952-2017. The simulated sediment load is represented by S^{sim}. The parameters *a*, *b*, *c*, and *d* were estimated by least-square method; 1984 is the year when the Wujiangdu Reservoir (the first large-scale reservoir built on the main stream of the WRB) was put into full operation, and also the year when the sediment load changed dramatically.

Model codes	The formulas of models
M1	$S^{sim} = a + b \cdot A + c \cdot I + d \cdot \mathrm{RI}$
M2	$S^{sim} = a \cdot (A)^{b} \cdot (I)^{c} \cdot (1 - \mathrm{RI})^{d}$
M3	$S^{sim} = a + b \cdot F_n + c \cdot \mathrm{RI}$
M4	$S^{sim} = a \cdot (F_n)^{b} \cdot (1 - \mathrm{RI})^{c}$
M5	$S^{sim} = \begin{cases} a + b \cdot F_n & t < 1984 \\ c + d \cdot \mathrm{RRCI}^{S} & t \geq 1984 \end{cases}$
M6	$S^{sim} = \begin{cases} a \cdot (F_n)^{b} & t < 1984 \\ c \cdot (1 - \mathrm{RRCI}^{S})^{d} & t \geq 1984 \end{cases}$
M7	$S^{sim} = \begin{cases} a + b \cdot F_n & t < 1984 \\ c + d \cdot \mathrm{RSTI} & t \geq 1984 \end{cases}$
M8	$S^{sim} = \begin{cases} a \cdot (F_n)^{b} & t < 1984 \\ c \cdot (1 - \mathrm{RSTI})^{d} & t \geq 1984 \end{cases}$

Table 4 Trend and change-point tests of hydrological series

Series	Mann-Kendall (MK) test		Pettitt (PT) test	
	Trend	p_{MK}	Breakpoint	p_{PT}
Rainfall (mm)	↓	0.236	1984	0.222
Runoff (10^8 m^3)	↓	0.507	2004	0.493
Sediment load (10^4 t)	↓	0.000	1984	0.000

Note: ↓ indicates a decreasing trend; p_{MK} and p_{PT} are the corresponding probability value of the Mann-Kendall test and Pettitt test, respectively. If p_{MK} or p_{PT} is less than 0.05, which means that there is a trend change or a change-point in the hydrological series at 5% significance level.

Table 5 Pearson linear correlation between rainfall characteristics and sediment load

Rainfall amount	Sediment load		Rainfall intensity	Sediment load	
	r	p_r		*r*	p_r
A_2	0.608	0.000	I_2	**0.420**	0.000
A_4	0.622	0.000	I_4	0.250	0.043
A_6	**0.623**	0.000	I_6	0.091	0.468
A_8	0.605	0.000	I_8	0.074	0.556
A_{10}	0.532	0.000	I_{10}	0.158	0.206
A_{15}	0.483	0.000	I_{15}	0.029	0.816
A_{20}	0.428	0.000	I_{20}	-0.029	0.818
A_{25}	0.314	0.010	I_{25}	0.009	0.943
A_{30}	0.218	0.079	I_{30}	0.075	0.552
A_{35}	0.196	0.115	I_{35}	0.111	0.374
A_{40}	0.209	0.093	I_{40}	0.099	0.431
A_{45}	0.134	0.284	I_{45}	0.007	0.954
A_{50}	0.122	0.328	I_{50}	0.055	0.660
A_{55}	0.120	0.335	I_{55}	0.120	0.335

Note: *r* denotes the Pearson correlation coefficient; p_r is the corresponding probability value of *r*, if it is less than 0.05, which means that there is a significant correlation between rainfall characteristic and sediment load.

Table 6 The results of *F* test and *t* test for eight regression models (the values shown in table are the corresponding probability values of *F* test and *t* test; *a*, *b*, *c*, and *d* are model parameters). *F* test is used for the testing of model validity, the significance of model parameters is tested by *t* test.

Model codes	*F* test	*t* test			
		a	*b*	*c*	*d*
M1	0.000	0.021	0.000	**0.340**	0.000
M2	0.000	0.005	0.000	**0.409**	0.000
M3	0.000	0.000	0.000	0.000	–
M4	0.000	0.005	0.000	0.000	–
M5	0.001	0.000	0.000	0.000	0.001
M6	0.000	0.000	0.000	0.000	0.000
M7	0.000	0.000	0.000	0.000	0.000
M8	0.000	0.000	0.000	0.000	0.000

Note: if the probability value of *F* test is less than 0.05, which means that the model passed the validity test, and model parameters are significant when probability values of *t* test are less than 0.05, and vice versa.

Table 7 The area and percentage of land use patterns

Land use pattern	1980		1990	
	Area (km^2)	Percentage (%)	Area (km^2)	Percentage (%)
Cropland	26686	30.353	27248	30.992
Forestland	45128	51.875	43945	50.513
Grassland	14886	17.112	15483	17.797
Water body	289	0.329	276	0.314
Urban land	283	0.322	326	0.371
Unused land	8	0.009	12	0.014

Figures

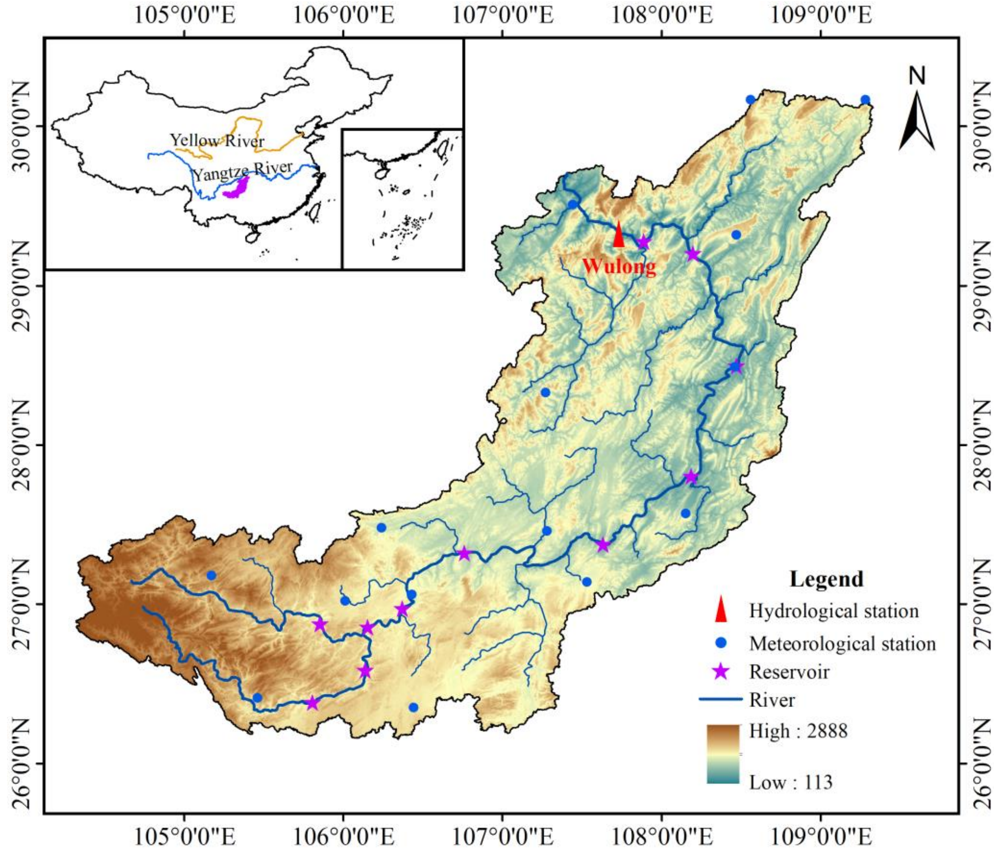

Figure 1 Location, hydro-meteorological stations and reservoirs of the Wujiang River Basin.

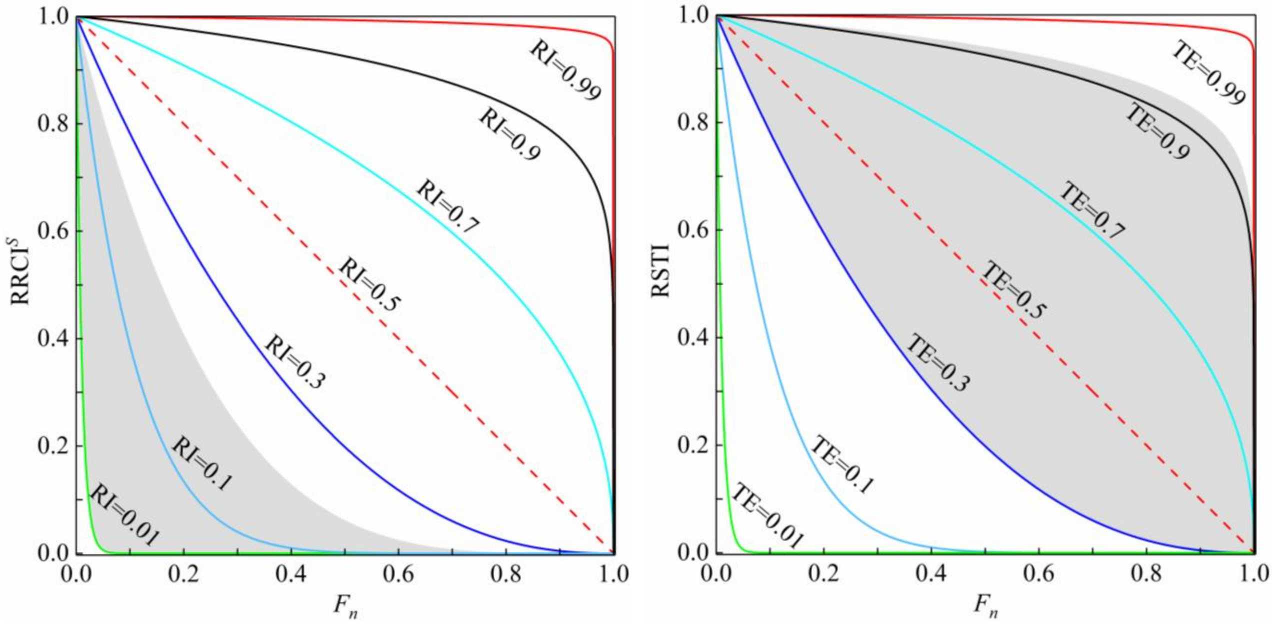

Figure 2 Relationship in Equation (9) and Equation (15). The left panel shows the relationship between reservoir index (RI), joint distribution function of rainfall amount and rainfall intensity (F_n) and rainfall-reservoir composite index (RRCI^S), the shaded area is the variation range of RI in the WRB (0.01-0.20); the right panel displays the relationship between sediment trapping efficiency (TE), joint distribution (F_n) and rainfall-augmented sediment trapping index (RSTI), the shaded area is the range of TE in the WRB (0.30-0.92).

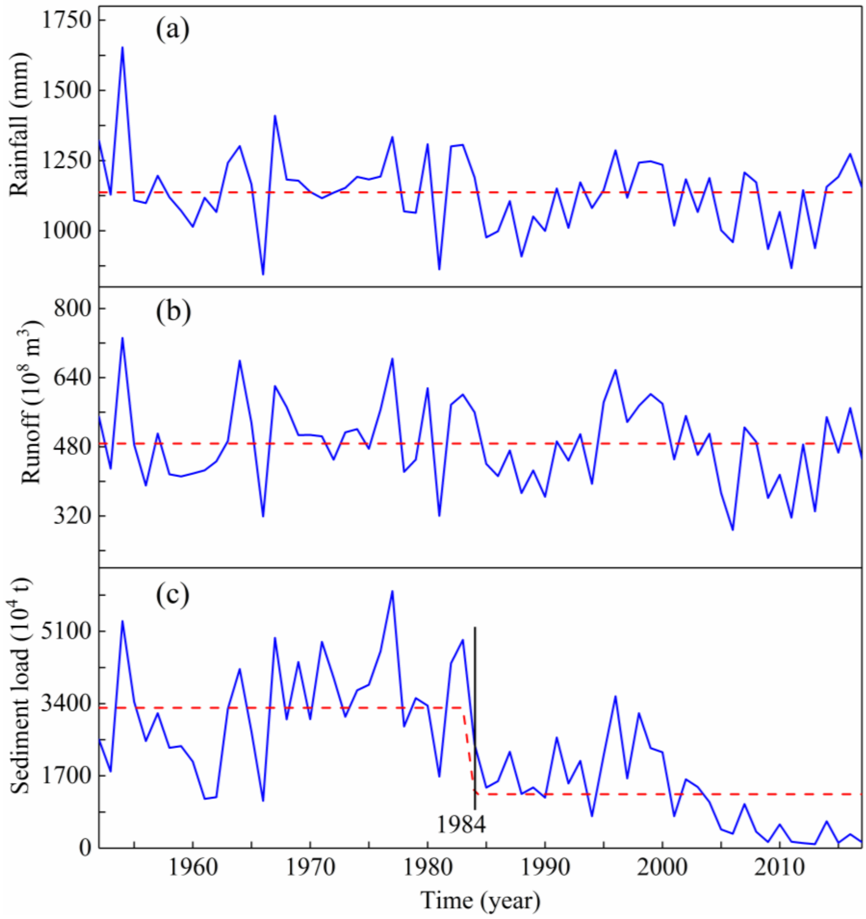

Figure 3 Time series of (a) annual rainfall, (b) annual runoff and (c) annual sediment load of the Wujiang River during 1952-2017. The dotted red line is the mean value of them.

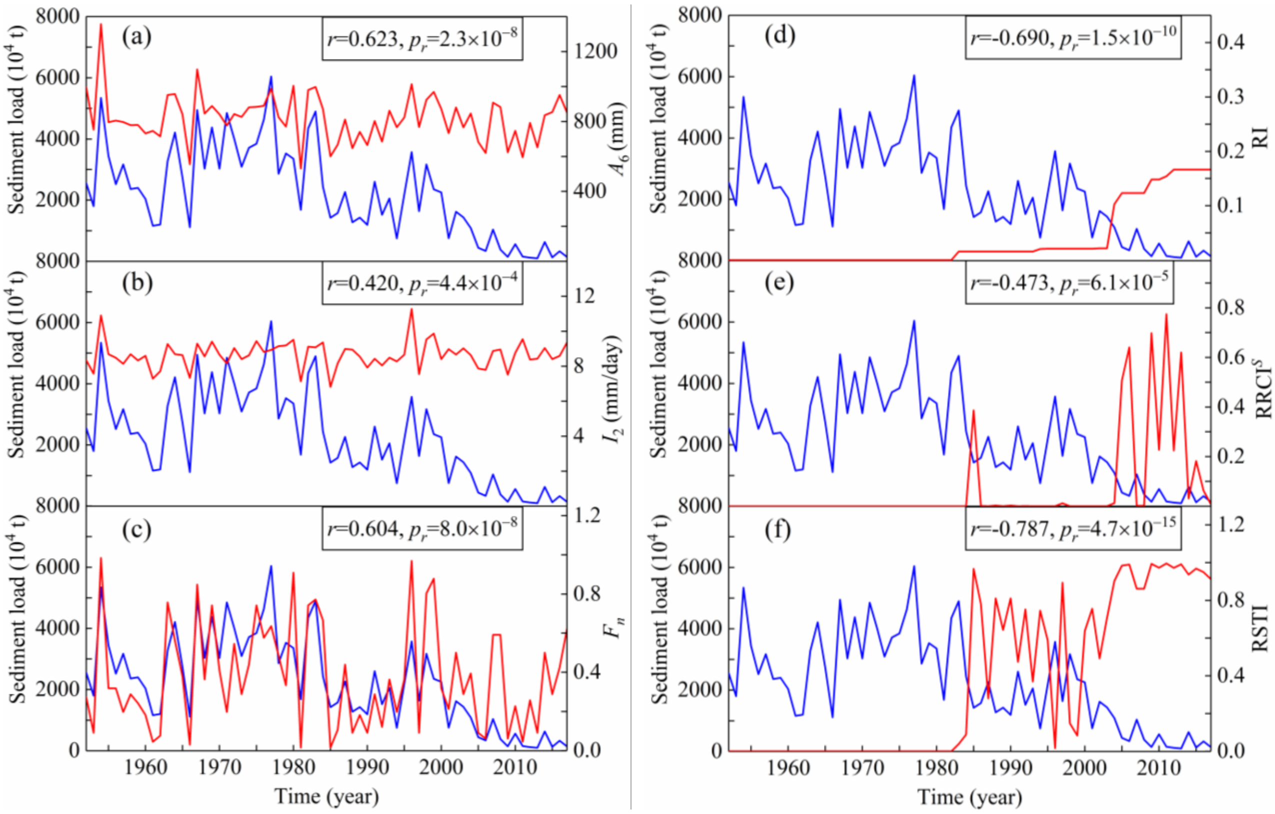

Figure 4 The time series of sediment load and explanatory variables (including: A_6, I_2, RI, F_n, RRCI^S, RSTI). The solid blue line represents observed sediment load and solid red line presents explanatory variables. And r denotes the Pearson correlation coefficient between sediment load and the explanatory variable; p_r is the corresponding probability value of r.

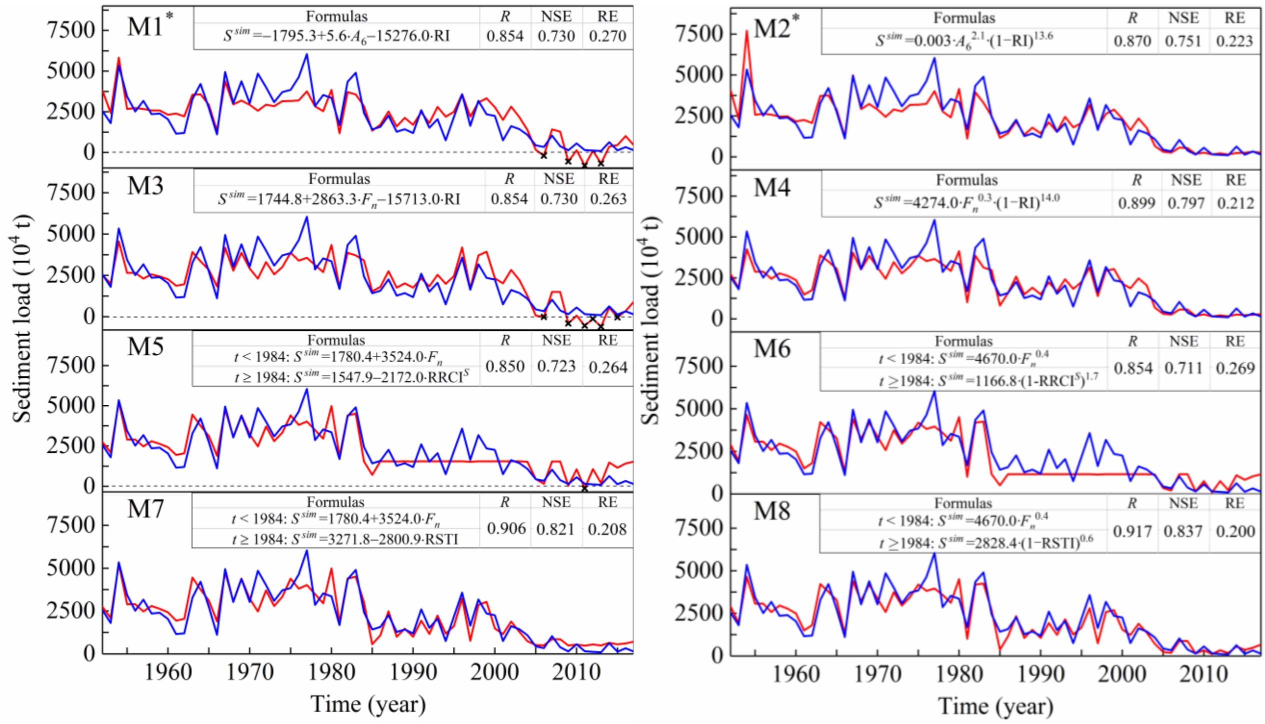

Figure 5 The time series of simulated sediment load (S^{sim}) of different regression models. The solid blue line represents the observed sediment load and solid red line denotes the simulated sediment load. The crosses in M1*, M3, M5 are negative values (or abnormal values) of simulated sediment load. M1* and M2* are improved models for M1 and M2 discussed in Section 4.3.

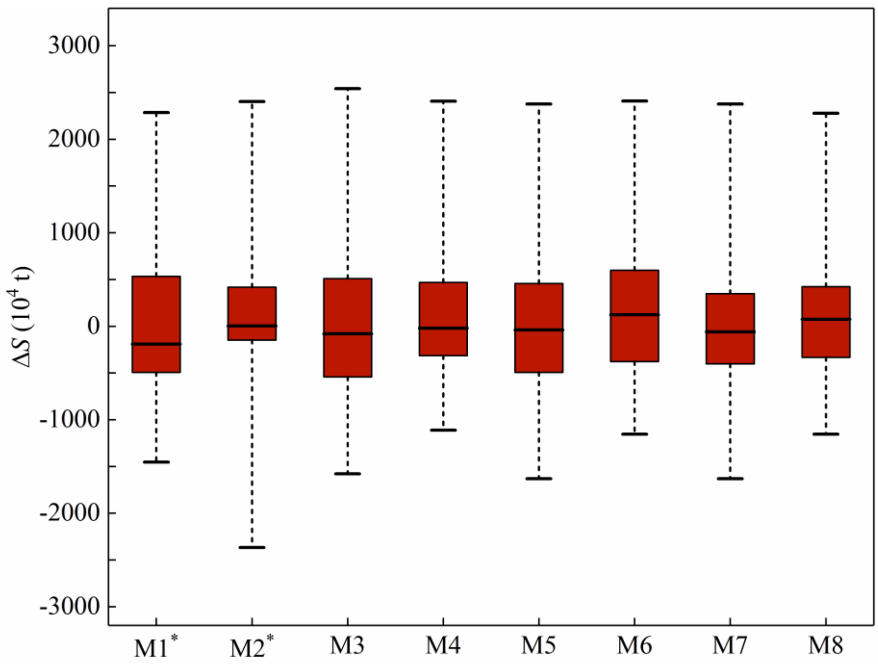

Figure 6 Box-plot of residuals (the difference between observed and simulated sediment load, namely Δ*S*) of eight regression models.

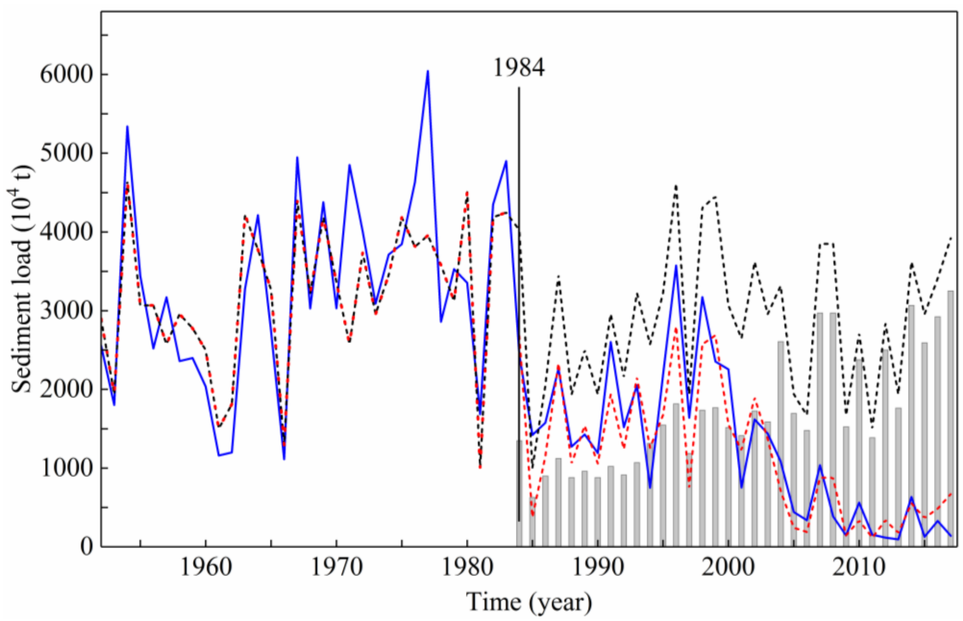

Figure 7 The time series of observed sediment load and simulated sediment load during 1952-2017. The solid blue line represents the observed sediment load. The dotted red line is the simulated sediment load by Equations (19a) and (19b), i.e. model M8. The dotted black line for the period of 1984-2017 is calculated by Equation (20), representing the sediment load caused by only rainfall under the assumption of no reservoirs. During 1984-2017, the difference between the dotted black line and the dotted red line is assumed to be the sediment load intercepted by reservoirs and displayed as gray columns.

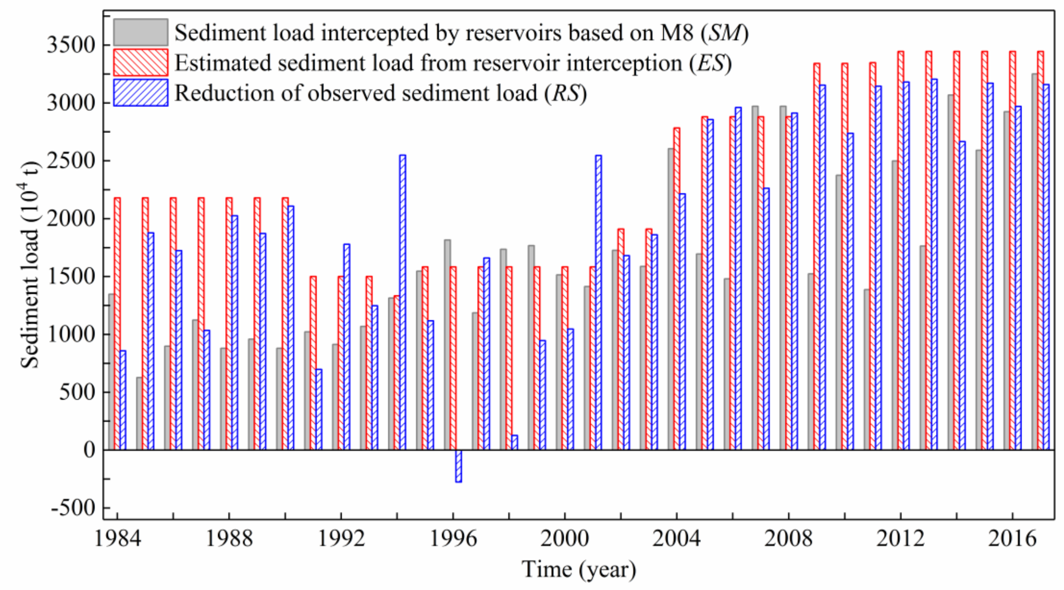

Figure 8 The sediment load intercepted by reservoirs based on M8 (*SM*), reduction of observed sediment load (*RS*) and estimated sediment load from reservoir interception (*ES*) during the period of 1984-2017 (the period after the change point 1984). *SM* is the difference between the dotted black line and the dotted red line for the period of 1984-2017 in Figure 7, *RS* is calculated by taking the difference between the mean value of sediment load from 1952 to 1983 (3299×10^4 t) and observed annual sediment load during 1984-2017. *ES* is computed by superposition of sediment trapping of all 11 reservoirs in Table 1.

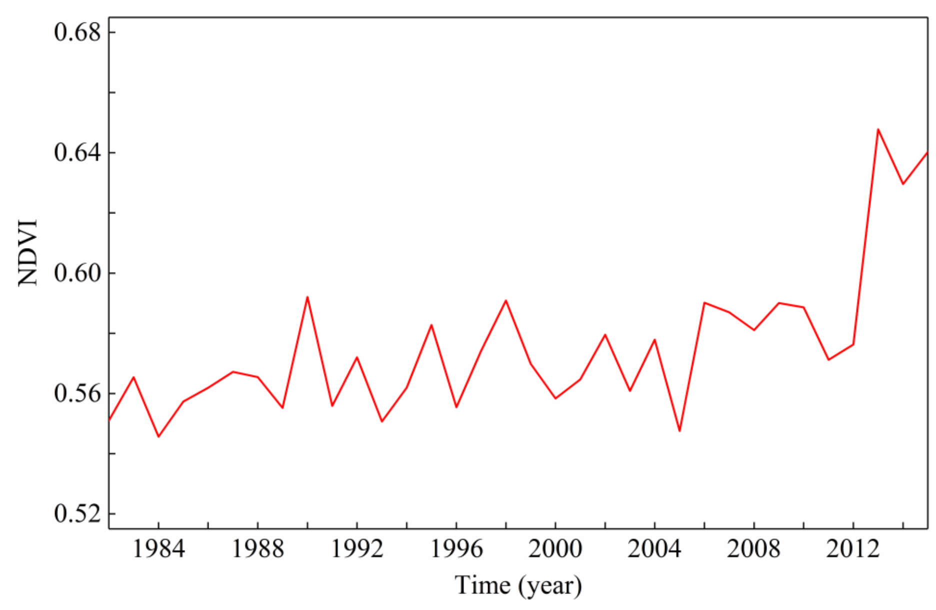

Figure 9 The time series of normalized difference vegetation index (NDVI) of the Wujiang River during 1982-2015.

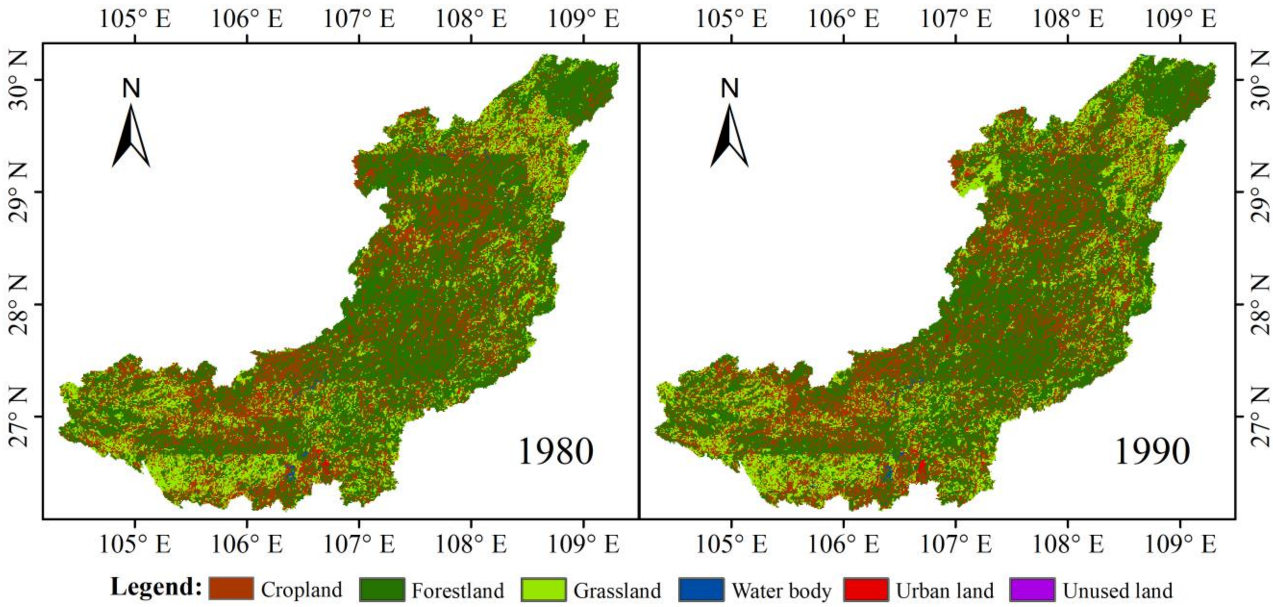

Figure 10 Land use and land cover change (LUCC) of the Wujiang River in 1980 and 1990.